



Full length article

# Nanofiber-based transforming growth factor- $\beta$ 3 release induces fibrochondrogenic differentiation of stem cells<sup>☆</sup>

Dovina Qu, Jennifer P. Zhu, Hannah R. Childs, Helen H. Lu<sup>\*</sup>

Biomaterials and Interface Tissue Engineering Laboratory, Department of Biomedical Engineering, Columbia University, 351 Engineering Terrace Building, MC 8904, 1210 Amsterdam Avenue, New York, NY 10027, United States

## ARTICLE INFO

## Article history:

Received 18 October 2018

Received in revised form 6 March 2019

Accepted 7 March 2019

Available online 9 March 2019

## Keywords:

Delivery

Nanofiber

Stem cells

Fibrocartilage

Interface

## ABSTRACT

Fibrocartilage is typically found in regions subject to complex, multi-axial loads and plays a critical role in musculoskeletal function. Mesenchymal stem cell (MSC)-mediated fibrocartilage regeneration may be guided by administration of appropriate chemical and/or physical cues, such as by culturing cells on polymer nanofibers in the presence of the chondrogenic growth factor TGF- $\beta$ 3. However, targeted delivery and maintenance of effective local factor concentrations remain challenges for implementation of growth factor-based regeneration strategies in clinical settings. Thus, the objective of this study was to develop and optimize the bioactivity of a biomimetic nanofiber scaffold system that enables localized delivery of TGF- $\beta$ 3. To this end, we fabricated TGF- $\beta$ 3-releasing nanofiber meshes that provide sustained growth factor delivery and demonstrated their potential for guiding synovium-derived stem cell (SDSC)-mediated fibrocartilage regeneration. TGF- $\beta$ 3 delivery enhanced cell proliferation and synthesis of relevant fibrocartilaginous matrix in a dose-dependent manner. By designing a scaffold that eliminates the need for exogenous or systemic growth factor administration and demonstrating that fibrochondrogenesis requires a lower growth factor dose compared to previously reported, this study represents a critical step towards developing a clinical solution for regeneration of fibrocartilaginous tissues.

## Statement of Significance

Fibrocartilage is a tissue that plays a critical role throughout the musculoskeletal system. However, due to its limited self-healing capacity, there is a significant unmet clinical need for more effective approaches for fibrocartilage regeneration. We have developed a nanofiber-based scaffold that provides both the biomimetic physical cues, as well as localized delivery of the chemical factors needed to guide stem cell-mediated fibrocartilage formation. Specifically, methods for fabricating TGF- $\beta$ 3-releasing nanofibers were optimized, and scaffold-mediated TGF- $\beta$ 3 delivery enhanced cell proliferation and synthesis of fibrocartilaginous matrix, demonstrating for the first time, the potential for nanofiber-based TGF- $\beta$ 3 delivery to guide stem cell-mediated fibrocartilage regeneration. This nanoscale delivery platform represents an exciting new strategy for fibrocartilage regeneration.

© 2019 Published by Elsevier Ltd on behalf of Acta Materialia Inc.

## 1. Introduction

Fibrocartilage is an essential tissue for musculoskeletal function and is commonly found in regions that are subjected to complex, multi-axial loads, including at ligament and tendon entheses

[1–3], the meniscus [4], the intervertebral disc [5,6], and the temporomandibular joint (TMJ) [7]. With an extracellular matrix comprised of proteoglycans and types I and II collagen [8–12], these tissues are tailored to withstand both tensile and compressive loads [13], such as those that develop between bone and ligament or tendon [14,15]. Structurally, the fibrocartilaginous interface connects the soft tissue to bone, minimizing stress concentrations and facilitating load transfer between these mechanically dissimilar tissues [1,2]. To enable integrative repair of soft tissues such as ligaments and tendons, there is significant interest in fibrocartilage regeneration strategies that will expedite healing and address this unmet clinical need.

<sup>☆</sup> Part of the Drug Delivery for Musculoskeletal Applications Special Issue, edited by Robert S. Hastings and Professor Johnna S. Temenoff.

<sup>\*</sup> Corresponding author at: Department of Biomedical Engineering, Columbia University, 351 Engineering Terrace Building, MC 8904, 1210 Amsterdam Avenue, New York, NY 10027, United States.

E-mail address: [hllu@columbia.edu](mailto:hllu@columbia.edu) (H.H. Lu).

To this end, mesenchymal stem cells (MSC) represent a promising cell source for fibrocartilage tissue engineering. These somatic progenitor cells are characterized by their high self-renewal and multi-lineage differentiation potential [16,17] and can be readily harvested from a variety of tissues throughout the body [18–22]. In particular, synovium-derived stem cells (SDSC) exhibit higher proliferative capacity and superior chondrogenic potential compared to stem cells from other tissue sources [23–25]. Resident SDSC have been shown to naturally increase proliferation, initiate chondrogenic differentiation, and migrate to the defect site following cartilage injury [26,27], while injected SDSC have been shown to promote meniscal regeneration in rabbit [28–30], rat [31,32], and porcine [33,34] models. It has also been reported that when compared to extra-articular stem cells, intra-articular stem cells share a more similar gene expression profile with other intra-articular cell types [35], suggesting that SDSC may be a favorable cell source for regeneration of intra-articular tissues such as enthesial or meniscal fibrocartilage.

Fibrochondrogenic differentiation of stem cells can be induced by administration of an appropriate combination of chemical and physical cues [36–41]. For instance, transforming growth factor (TGF)- $\beta$  is a family of pleiotropic cytokines that regulate cell growth, differentiation, tissue repair and inflammation, and are essential for fibrocartilage and cartilage formation [42–45]. Media supplementation with TGF- $\beta$ 1 has been reported to enhance cell proliferation as well as collagen and proteoglycan synthesis in explanted fibrocartilage tissues [46–49]. For fibrochondrocyte-seeded scaffolds, TGF- $\beta$ 1 and TGF- $\beta$ 3 media supplementation have similarly been shown to increase collagen synthesis, leading to improved functional properties [50–52]. Interestingly, media supplementation with TGF- $\beta$ 3 has been shown to facilitate fibrocartilage formation by bone marrow-derived stem cells (BMSC) seeded on polymer nanofibers [36,37].

However, effective protein delivery remains a challenge for clinical application of growth factor-based tissue regeneration strategies. Current methods often rely on systemic or bolus injection, but administered growth factors can rapidly diffuse away from the target tissue and cause undesirable side effects. Given the pleiotropic effects of the TGF- $\beta$  family of proteins, it is especially important to ensure controlled, localized delivery to only the targeted cells or tissues. This study focuses on the design and optimization of a nanofiber scaffold system that provides both structural and chemical inductive cues for SDSC-mediated fibrocartilage regeneration. Specifically, the inductive factor of interest is TGF- $\beta$ 3, as it is expressed at the enthesis during fetal development [53], accelerates healing and improves functional outcomes in tendon-to-bone repair [54], and plays a role in fibrocartilaginous metaplasia of tendon matrix in response to compressive loading [55]. Recently, co-release of TGF- $\beta$ 3 and connective tissue growth factor (CTGF) from polymer microspheres embedded in a 3D-printed microfiber matrix has been reported to guide meniscal [56] and TMJ [57] fibrocartilage formation.

This study explores the design of a nanofiber-based delivery system for several reasons. Nanofibers are ideal for regenerating the narrow interface between ligaments and bone, as they are designed to structurally recapitulate the native collagen alignment and mechanical properties of ligaments and tendon [58,59]. Moreover, inductive factors, such as nerve growth factor [60,61], platelet-derived growth factor [62], or TGF- $\beta$ 1 [63,64], can be readily incorporated into nanofibers during electrospinning, which allows for a simplified and more streamlined fabrication process. The higher effective surface area-to-volume ratio exhibited by nanofibers is also more favorable for release, and enables greater interaction between seeded cells and the encapsulated biomolecules. It is thus hypothesized that local delivery of TGF- $\beta$ 3 from nanofibers will enhance SDSC proliferation and induce the synthe-

sis of a fibrocartilage-like matrix, comprising types I and II collagen as well as proteoglycans. Given that the concentration of administered TGF- $\beta$ 3 can differentially affect activation of downstream signaling pathways in synovial fibroblasts [65], the effects of both low- and high-dose delivery systems will also be evaluated. This nanoscale delivery platform represents an exciting new strategy for fibrocartilage interface regeneration, and it is anticipated that findings from this study will have broader impact and relevance for guiding the regeneration of other key fibrocartilaginous tissues.

## 2. Materials and methods

### 2.1. Scaffold fabrication

Aligned protein-containing polymer blend fibers of poly- $\epsilon$ -caprolactone (PCL) and polylactide-co-glycolide (PLGA) were fabricated by electrospinning [66]. For PCL-PLGA scaffolds, PCL ( $M_w \sim 70,000$ – $90,000$ ; Sigma-Aldrich) and PLGA (85:15,  $M_w \sim 123.6$  kDa; Evonik) were dissolved at a 5:1 weight to volume (w/v) ratio in a 3:2 v/v solution of dichloromethane (Sigma-Aldrich) and N,N-dimethylformamide (Sigma-Aldrich), resulting in an 18% w/v polymer solution. As co-encapsulation of bovine serum albumin (BSA) has been reported to stabilize incorporated growth factor during the electrospinning process [60,61,67], up to 10% w/w of finely ground BSA (Sigma-Aldrich) was added to the polymer solution and then vortexed for 1 h. Next, TGF- $\beta$ 3 (Sigma-Aldrich) was reconstituted in deionized water (1  $\mu\text{g}/\mu\text{L}$ ) and added to the PCL-PLGA/BSA mixture (10  $\mu\text{g}$  for low-dose and 20  $\mu\text{g}$  for high-dose), and then vortexed for an additional hour. The PCL-PLGA/BSA/TGF- $\beta$ 3 mixture was then loaded into a 5 mL syringe fitted with an 18G stainless steel blunt-tip needle, and was electrospun at 11–13 kV. To form aligned meshes, the solutions were dispensed at 1 mL/hour using a syringe pump (Harvard Apparatus) over a distance of 12 cm onto a grounded rotating (20 m/s) mandrel.

Fiber morphology and diameter of as-fabricated meshes were examined by secondary scanning electron microscopy (SEM; 2 kV, Hitachi 4700, Hitachi Ltd.). Briefly, samples were pre-coated with gold-palladium to reduce surface charging effects (Sputter Coater 108 Auto, Cressington Scientific). Fiber diameter was quantified via image analysis of SEM micrographs (2500 $\times$ ,  $n = 5$  images/group; 10 random fibers/image, ImageJ, NIH) [68].

### 2.2. TGF- $\beta$ 3 release kinetics and modeling

Growth factor incorporation efficiency and bioactivity post-electrospinning were determined. Briefly, as-fabricated TGF- $\beta$ 3 meshes (thickness:  $90 \pm 10$   $\mu\text{m}$ ,  $\phi = 8$  mm,  $n = 5$ /group) were dissolved in a 1:2 solution of chloroform (Fisher) and Dulbecco's Modified Eagle's Medium (DMEM, Cellgro-Mediatech) supplemented with 1.25 mg/mL BSA. This solvent mixture was customized to maximize the recovery of TGF- $\beta$ 3. The mixtures were vortexed for 30 min and then centrifuged at 20,000 RCF for 5 min to separate the organic and aqueous phases. The amount of TGF- $\beta$ 3 in the aqueous phase was measured by ELISA (R&D Systems), following the manufacturer's suggested protocol.

To assess TGF- $\beta$ 3 release kinetics, as-fabricated TGF- $\beta$ 3 meshes (thickness:  $90 \pm 10$   $\mu\text{m}$ ,  $\phi = 10$  mm,  $n = 5$ /group) were sterilized by ultraviolet irradiation (15 min/side) and then incubated in DMEM supplemented with 1.25 mg/mL BSA, 2% penicillin/streptomycin (P/S, Cellgro-Mediatech), 0.2% amphotericin B (amp-B, Cellgro-Mediatech), and 0.2% gentamicin sulfate (G/S, Cellgro-Mediatech). All samples were incubated in 1 mL media (scaffold weight-to-media volume ratio: low-dose:  $1.29 \pm 0.14$  mg/mL; high-dose:  $1.53 \pm 0.10$  mg/mL), which was sufficient to achieve and maintain perfect sink conditions, and maintained at 37  $^{\circ}\text{C}$  in humidified

conditions. At each time point (0, 0.25, 0.5, 1, 4, 7, 11, and 14 days), media from each sample was collected and replaced with fresh media. Media TGF- $\beta$ 3 concentrations were measured by ELISA. In order to better understand the mechanism of release, the experimental release data was fit to the model developed by Ritger and Peppas [69], which describes solute release from non-swellable polymeric delivery devices of various geometries. Assuming one-dimensional release under perfect sink conditions, the release from a monodispersion of cylinders is described by:

$$\frac{M_t}{M_\infty} = kt^n \quad (1)$$

where  $M_t/M_\infty$  is the fractional release at time  $t$ ,  $k$  is a constant, and  $n$  is the diffusional exponent.

### 2.3. Cell isolation

Following published protocols [70], SDSC were harvested from bovine knee joints. Briefly, neonatal (1–7 days old) bovine tibiofemoral joints were obtained from a local abattoir ( $n = 2$ , tissues pooled; Green Village Packing Company). Prior to harvest, joints were sterilized by soaking in soapy water for 40 min, followed by 70% ethanol for 20 min, after which the surrounding muscle and subcutaneous fascia were removed. The joint capsules were then opened aseptically in a sterile environment, and the synovial membrane lining the femoral condyles was harvested. The synovial tissue was digested for 4 h at 37 °C with collagenase II (1.2% w/w; Worthington Biochemical) in Minimum Essential Medium Alpha ( $\alpha$ MEM; Cellgro-Mediatech) supplemented with 10% fetal bovine serum (FBS), 2% P/S, 0.2% Amp-B, and 0.2% G/S. The mixture was then filtered (30  $\mu$ m, Spectrum Labs), and the isolated cells were collected by centrifugation and plated at a density of  $1.8 \times 10^3$  cells/cm<sup>2</sup> on tissue culture plastic. Cells were maintained in fully-supplemented (F/S)  $\alpha$ MEM containing 10% FBS, 1% P/S, 1% non-essential amino acids (NEAA; Cellgro-Mediatech), 0.1% Amp-B, and 0.1% G/S, under humidified conditions at 37 °C and 5% carbon dioxide.

To eliminate synovium-derived macrophages and obtain a pure population of SDSC, cells were subsequently cultured for 4 passages [71] by splitting confluent cells in each passage at a ratio of 1:4. Passage 4 SDSC were used for all subsequent characterization and differentiation studies. This process has been shown to yield a population of cells that is positive for mesenchymal stem cell marker CD73 and negative for hematopoietic cell marker CD34 [72]. To confirm the stemness of the isolated cells, their adipogenic [17], osteogenic [73], and chondrogenic [74] differentiation potential were evaluated following established protocols. For adipogenic ( $n = 3$ ) and osteogenic ( $n = 3$ ) differentiation, SDSC were plated at a density of 100 cells/cm<sup>2</sup> and cultured in F/S  $\alpha$ MEM for 10 days. For adipogenic differentiation, the medium was then replaced with F/S DMEM supplemented with 1  $\mu$ M dexamethasone (Sigma-Aldrich), 500  $\mu$ M isobutyl-1-methyl-xanthine (Sigma-Aldrich), 100  $\mu$ M indomethacin (Sigma-Aldrich), and 10  $\mu$ g/mL insulin (Sigma-Aldrich). After an additional 14 days of culture, cells were fixed in 10% neutral-buffered formalin (NBF) and stained with Oil Red-O (0.18% solution, Sigma-Aldrich). For osteogenic differentiation, the medium was replaced with F/S low-glucose DMEM (Gibco) supplemented with 10 mM  $\beta$ -glycerolphosphate (Sigma-Aldrich), 0.1  $\mu$ M dexamethasone, and 200  $\mu$ M ascorbic acid (Sigma-Aldrich). After an additional 14 days of culture, cells were fixed in 10% NBF and stained with von Kossa (5% silver nitrate solution, Fisher Scientific). For chondrogenic differentiation ( $n = 3$ ), cells were pelleted by centrifugation ( $2 \times 10^5$  cells/pellet) and cultured in DMEM supplemented with antibiotics, 1% ITS+ (Corning), 50  $\mu$ g/mL L-proline (Sigma-Aldrich), 0.1  $\mu$ M dexamethasone, 50  $\mu$ g/mL ascorbic acid, and 10 ng/mL TGF- $\beta$ 3 for 21 days. Pellets

were then fixed in 10% NBF, embedded in paraffin, cut into 7  $\mu$ m sections, and stained with Alcian blue (1% solution, Sigma-Aldrich).

### 2.4. Cell culture

Scaffold discs (thickness:  $90 \pm 10$   $\mu$ m,  $\phi = 10$  mm) were sterilized by ultraviolet radiation (15 min/side). Prior to cell seeding, scaffolds were incubated in DMEM supplemented with 20% FBS, 2% P/S, 0.2% amp-B, and 0.2% G/S overnight at 37 °C to enhance cell attachment. The cells were seeded onto control (BSA only), low-dose TGF- $\beta$ 3, or high-dose TGF- $\beta$ 3 scaffolds at a density of  $3 \times 10^4$  cells/cm<sup>2</sup>, and were cultured in F/S DMEM, with media exchange occurring every 3 to 4 days. Cells cultured on control scaffolds with and without exogenous supplementation of TGF- $\beta$ 3 served as controls. Based on the mean amount of available TGF- $\beta$ 3 in the high-dose scaffold group in the first week of culture, the cell culture media of the exogenous TGF- $\beta$ 3 group was supplemented with 200 pg/mL TGF- $\beta$ 3 at every feeding. To evaluate the rate of growth factor consumption, media samples were collected at every feeding and TGF- $\beta$ 3 amount was quantified by ELISA. Cell viability, proliferation, mineralization potential, and matrix deposition on the scaffolds were evaluated at 1, 7, 14, and 28 days.

### 2.5. Cell viability and proliferation

At each time point, cell viability ( $n = 3$ ) was assessed by Live/Dead staining (Invitrogen) according to the manufacturer's suggested protocol. Briefly, samples were rinsed with phosphate-buffered saline (PBS; Sigma-Aldrich), stained, and then imaged by confocal microscopy (Fluoview FV1000, Olympus) at 488 nm and 594 nm to assess cell viability and death, respectively.

Cell proliferation ( $n = 5$ ) was measured by quantifying the amount of DNA in each sample (Quant-iT PicoGreen dsDNA Assay, Invitrogen). Briefly, at each time point, samples were rinsed with PBS and then homogenized with 0.1% Triton-X (Sigma-Aldrich). Samples were subjected to 15 s of ultrasonication at 5 W. Fluorescence was measured at 485 nm excitation and 535 nm emission wavelengths (SpectraFluor Plus, Tecan). Measured fluorescence intensity was correlated to a DNA standard curve, and a conversion factor of 7.7 pg DNA/cell was then used to determine total cell number in each sample.

### 2.6. SMAD activation

To evaluate downstream effects of TGF- $\beta$ 3 released from the scaffolds, activation of phosphorylated SMAD (pSMAD) 2/3 and pSMAD 1/5/9 after 24 h of culture was evaluated by whole-mount immunohistochemistry. Briefly, samples harvested on day 1 were fixed immediately in 10% NBF and then rinsed briefly in PBS and transferred onto glass slides. Samples were incubated overnight at 4 °C with antibodies for pSMAD 2/3 ( $n = 3$ ; 8828, Cell Signaling Technology) or pSMAD 1/5/9 ( $n = 3$ ; 13820, Cell Signaling Technology), which were diluted 1:200 and 1:800, respectively, in serum-free Protein Block (Dako Cytomation) prior to use. After a PBS wash, a FITC-conjugated secondary antibody (ab6798, Abcam) diluted 1:200 in Protein Block was added, and samples were incubated for an additional hour at room temperature. Cell nuclei were counterstained with DAPI (Sigma-Aldrich). Samples were imaged using a confocal microscope with a 495 nm excitation wavelength.

### 2.7. Matrix synthesis

Total proteoglycan ( $n = 5$ ) and collagen ( $n = 5$ ) content were quantified using a modified 1,9-dimethylmethylene blue (DMMB) dye-binding assay [75,76] and the hydroxyproline assay [77], respectively. Sample lysates were dehydrated and then subjected

to an 18 h digestion in papain buffer (Sigma-Aldrich) to solubilize matrix proteins. For proteoglycan quantification, samples were mixed with DMMB dye (pH 3.5, Sigma-Aldrich) and absorbance was immediately measured ( $\mu$ Quant, Bio-Tek) at both 540 nm and 595 nm. Proteoglycan content was determined by correlating measured absorbance to a chondroitin-6-sulfate standard curve. For collagen quantification, samples were hydrolyzed in 2 N sodium hydroxide (Sigma-Aldrich) and subsequently incubated with Chloramine-T solution (Sigma-Aldrich) and Ehrlich's reagent [77]. Absorbance was measured (SpectraFluor Plus) at 555 nm and collagen content of each sample was determined by correlating measured optical density to a collagen standard curve.

Total proteoglycan ( $n = 2$ ) and collagen ( $n = 2$ ) were also visualized by Alcian blue and Picrosirius red (0.1% solution, Sigma-Aldrich) staining, respectively, of frozen sections. Samples harvested on day 28 were fixed immediately in 10% NBF supplemented with 1% cetylpyridinium chloride (CPC; Sigma-Aldrich) to preserve proteoglycans [78,79]. Following fixation, samples were embedded in 5% poly(vinyl alcohol) (PVA; Sigma-Aldrich), and 10  $\mu$ m sections spanning the entire thickness of the scaffold were obtained using a cryostat (Hacker-Bright OTF, Hacker Instruments and Industries). Stained sections were imaged by light microscopy (Axiovert 25, Zeiss).

Deposition of type I ( $n = 2$ ) and type II collagen ( $n = 2$ ) was evaluated by immunohistochemistry [80]. Sample sections were incubated overnight at 4 °C with antibodies for type I (ab90395, Abcam) or type II collagen (ab34712, Abcam), which were diluted 1:100 in serum-free Protein Block prior to use. After a PBS wash, FITC-conjugated secondary antibodies (type I collagen: ab6785, Abcam; type II collagen: ab6798, Abcam) diluted 1:200 in Protein Block were added, and samples were incubated for an additional hour at room temperature. Cell nuclei were counterstained with DAPI. Samples were imaged using a confocal microscope with a 495 nm excitation wavelength.

## 2.8. Gene expression

The expression of fibrocartilage-related markers was assessed via quantitative real-time reverse transcriptase polymerase chain reaction (qPCR,  $n = 5$ /group) after 1 and 28 days of culture. Total RNA was isolated using the Trizol extraction method (Invitrogen). Isolated RNA was then reverse-transcribed into complementary DNA using the SuperScript First-Strand Synthesis System (Invitrogen), and the cDNA product was amplified using recombinant Taq DNA polymerase (Invitrogen). The following oligonucleotide primer sequences were used: GAPDH: GCTGGTGCTGAGTATGTGGT (sense), CAGAAGGTGCAGAGATGATGA (anti-sense); type I collagen: CTTCTGGAGCAAGTGGTGAA (sense), GATCCTTCAGCACCAGGAG (anti-sense); type II collagen: GCATTGCCTACCTGGACGAA (sense), GAACCTGCTGTGGCCTCAG (anti-sense); TGF- $\beta$ 3: CTTCACGTGTCC TCAGTGG (sense), GGAAGAGCTCAATCCTCTGC (anti-sense); aggrecan: GTGAATCCAAAACGCCACT (sense), CGGCGTAGCACTGTCCAG (anti-sense). GAPDH served as the house-keeping gene. All genes were amplified for 50 cycles in a thermocycler (Bio-Rad iCycler) with a fluorescent probe (SYBR Green, Invitrogen). Quantitative analysis of gene expression was performed using the delta-delta CT method.

## 2.9. Statistical analysis

Results are presented as mean  $\pm$  standard deviation. Two-way analysis of variance (ANOVA) was performed to determine time- and culture condition-dependent differences in growth factor release, cell proliferation, matrix production or gene expression. The Tukey-Kramer post-hoc test was used for all pair-wise comparisons ( $p < 0.05$ ). All statistical analyses were performed using JMP IN (4.0.4, SAS Institute).

## 3. Results

### 3.1. Scaffold characterization

To assess the protective effects of BSA, aligned PCL-PLGA scaffolds with two concentrations of BSA and TGF- $\beta$ 3 were fabricated via electrospinning. Growth factor release from PCL-PLGA fibers was shown to increase as a function of BSA incorporation, with meshes that contained 10% BSA exhibiting approximately three-fold higher release over 15 days compared to meshes with only 5% BSA (Fig. 1A). Based on these results, all subsequent studies were conducted using PCL-PLGA meshes with 10% BSA incorporated.

Evaluation of fiber morphology showed no significant difference in fiber diameter among control (10% BSA-only), low-, and high-dose TGF- $\beta$ 3 scaffold groups (Fig. 1A, C). Growth factor incorporation was evaluated by ELISA, with an incorporation efficiency of  $46.0 \pm 2.5\%$  measured in low-dose scaffolds and  $41.7 \pm 2.5\%$  in high-dose scaffolds (Fig. 1C). Based on evaluation of as-fabricated meshes, each low-dose sample used for cell culture contains on average  $6.0 \pm 0.3$  ng of TGF- $\beta$ 3, while high-dose samples contained  $12.7 \pm 0.4$  ng TGF- $\beta$ 3.

Evaluation of TGF- $\beta$ 3 release showed an initial burst release of TGF- $\beta$ 3 within the first six hours of incubation, followed by slower, sustained release (Fig. 1D). Over the course of 14 days, high-dose scaffolds released  $2.6 \pm 0.2\%$  of total incorporated TGF- $\beta$ 3, which was approximately two-fold higher than the total cumulative release from the low-dose scaffolds (Fig. 1C, E).

### 3.2. Cell viability and proliferation

Stem cells isolated from the synovium were adherent to tissue culture plastic and exhibited multi-lineage osteogenic, adipogenic, and chondrogenic differentiation potential characteristic of MSC (Suppl. Fig. 1). Cells seeded on the nanofiber scaffolds remained viable in all groups (Fig. 2A) and proliferated significantly over time (Fig. 2B). By day 7, cell number was significantly higher for the two TGF- $\beta$ 3-releasing scaffold groups when compared to the control and the exogenously stimulated groups. At day 14, the highest cell number was found in the high-dose TGF- $\beta$ 3 scaffold group and in the exogenous group. No significant differences in cell number were observed among groups by day 28. Cells were observed to penetrate through the scaffold depth in all groups by day 28 (Suppl. Fig. 2).

### 3.3. TGF- $\beta$ 3-Mediated cell signaling

Within the first day of culture, the presence of pSMAD 2/3 and pSMAD 1/5/9 were detected within and surrounding the nuclei of cells cultured on high-dose TGF- $\beta$ 3 scaffolds (Fig. 2C; Suppl. Fig. 3). In contrast, little to no prominent staining for pSMADs was observed in the control or exogenously stimulated groups.

### 3.4. Proteoglycan deposition

All groups supported proteoglycan deposition by SDSC (Fig. 3A), with increasing glycosaminoglycan (GAG) synthesis evident over time for all groups that were exposed to TGF- $\beta$ 3 (Fig. 3B). Synthesis of GAG was significantly higher on the TGF- $\beta$ 3 scaffolds compared to control scaffolds from day 7 onwards. Moreover, a dose-dependent response was observed, with consistently higher proteoglycan content detected on high-dose compared to low-dose scaffolds. While GAG deposition in the exogenous group was initially lower than in the TGF- $\beta$ 3 scaffold groups, by day 28, the highest GAG content was found in the exogenous group. Histological analysis showed that proteoglycans were deposited throughout

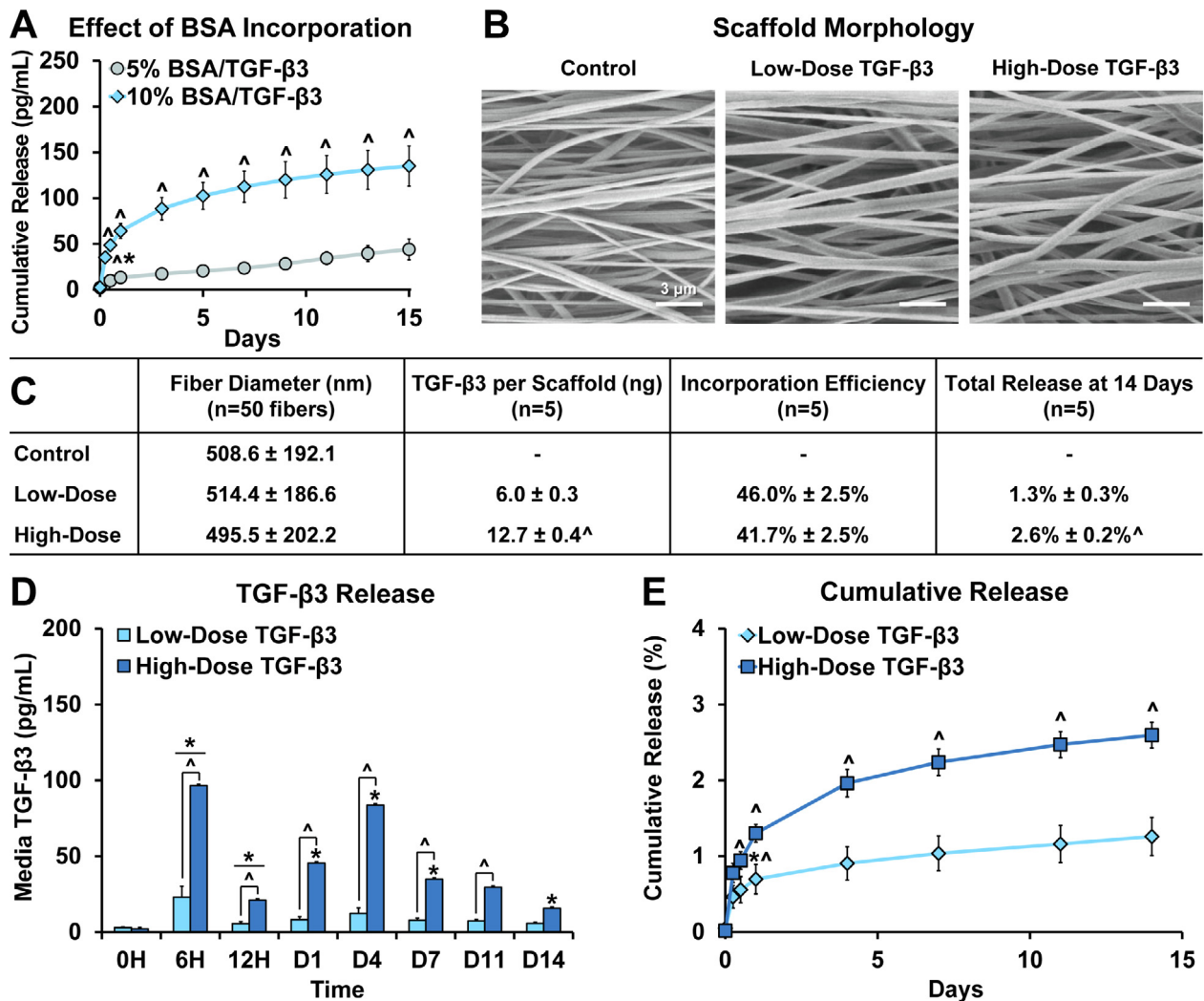


**Fig. 1.** TGF- $\beta$ 3 scaffold characterization. (A) TGF- $\beta$ 3 release from PCL-PLGA nanofibers was modulated by changing the concentration of co-incorporated BSA, with significantly more bioactive TGF- $\beta$ 3 released from the 10% BSA meshes ( $n = 5$ ;  $^{\wedge}p < 0.05$ ). (B) Aligned PCL-PLGA nanofibers containing 10% BSA, with and without TGF- $\beta$ 3 were fabricated by electrospinning. (C) Evaluation of TGF- $\beta$ 3 content and scaffold morphology of as-fabricated meshes showed that the high-dose group contained approximately double the amount of TGF- $\beta$ 3 as the low-dose group ( $n = 5$ ;  $^{\wedge}p < 0.05$ ), and no significant difference in fiber diameter or growth factor incorporation efficiency between groups. (D) Growth factor release was detected within the first 6 h of incubation, and (E) sustained release of TGF- $\beta$ 3 was observed from both low- and high-dose meshes over the 14-day period ( $n = 5$ ;  $^{\wedge}p < 0.05$ ). Note:  $^{\wedge}p < 0.05$ , different from previous time point;  $^{\wedge}p < 0.05$ , difference between groups.

the scaffold in all groups, with strong staining at the top and bottom surfaces of the scaffold (Fig. 3A).

### 3.5. Collagen deposition

All scaffold groups supported deposition of collagen by SDSC (Fig. 3A). There were no significant differences in total collagen deposition among the control and TGF- $\beta$ 3-releasing scaffold groups (Fig. 3C). However, collagen deposition in the exogenous, continuously stimulated group was significantly higher than in the control and low-dose scaffold groups at day 28. Histological analysis showed that collagen matrix was distributed throughout the scaffold, and polarized light imaging revealed that collagen deposition followed the alignment of the underlying nanofiber scaffold (Fig. 3A). Examination of the collagenous matrix by immunohistochemistry showed that both type I and type II collagen were deposited in the groups that were exposed to TGF- $\beta$ 3, while type I collagen, but not type II collagen, was observed on control scaffolds (Fig. 3A).

### 3.6. Gene expression

After 24 hours of culture, expression of TGF- $\beta$ 3 was significantly downregulated on TGF- $\beta$ 3-loaded scaffold groups compared to both the growth factor-free and the exogenously stimulated controls (Fig. 4; Suppl. Fig. 5). Expression of type I collagen and aggrecan were also significantly upregulated in the exogenous TGF- $\beta$ 3 groups compared to control and TGF- $\beta$ 3 scaffold groups on day 1. While type II collagen expression was not detectable on day 1, it was upregulated by day 28 and found to be similar among all groups. At day 28, aggrecan expression was significantly upregulated on TGF- $\beta$ 3 scaffolds compared to the control and exogenous groups, while type I collagen expression was significantly downregulated in the exogenous group compared to all other groups.

### 3.7. TGF- $\beta$ 3 release and consumption

Fitting the cumulative TGF- $\beta$ 3 release data to the Ritger-Peppas model for release (Eq. (1)), the fractional release from low-dose scaffolds can be described by (Fig. 5A):

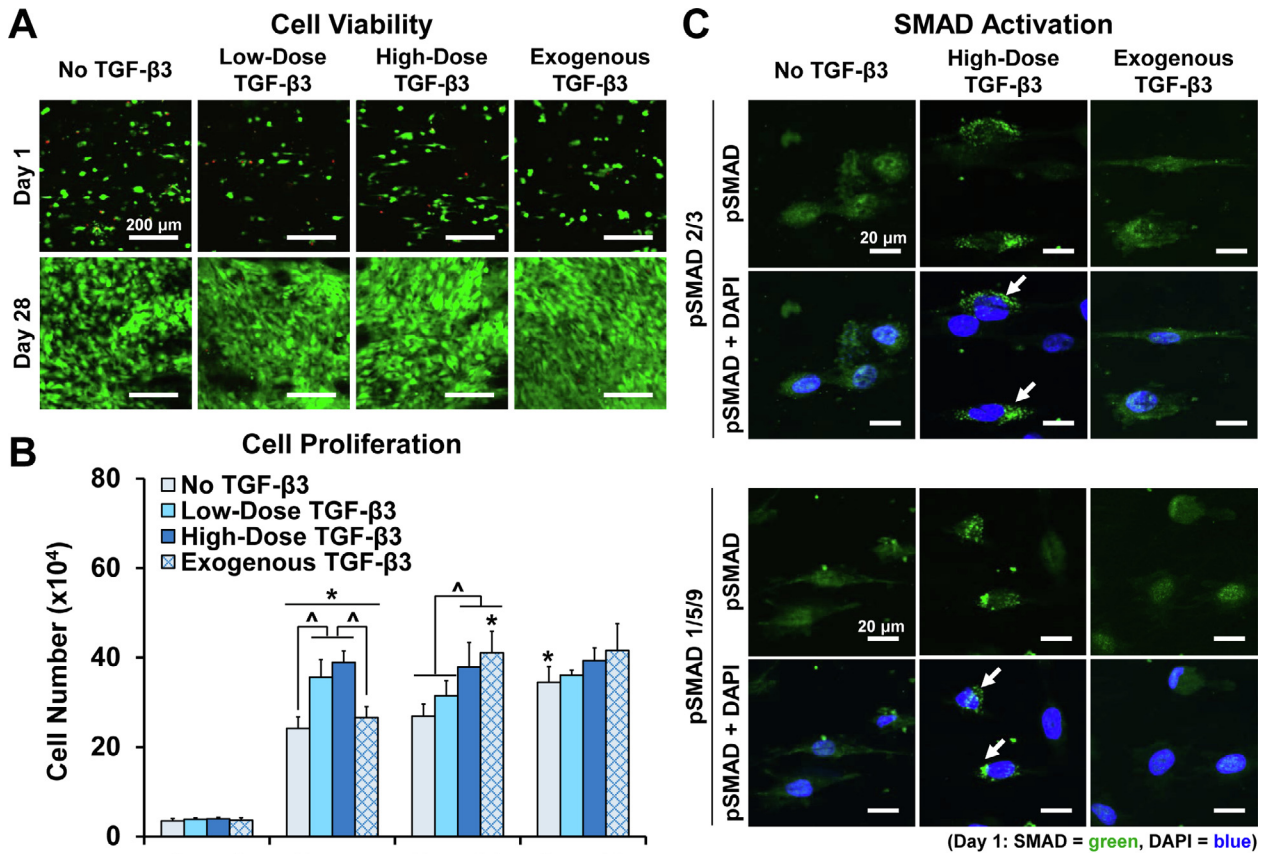


**Fig. 2.** SDSC proliferation and activation of downstream TGF- $\beta$ 3 signaling. (A) SDSC seeded on TGF- $\beta$ 3-releasing scaffolds remained viable and proliferated over time, with (B) significantly higher initial cell proliferation on TGF- $\beta$ 3 scaffolds compared to growth factor-free negative control and media addition of TGF- $\beta$ 3 (exogenous, positive control) at day 7 ( $n = 5$ ;  $^* p < 0.05$ , between consecutive time points;  $^* p < 0.05$ , between groups). Note: compared to the high-dose group, cells in the exogenous group are exposed to approximately 2.5 $\times$  and 5 $\times$  more TGF- $\beta$ 3 by day 14 and day 28, respectively. (C) Within the first 24 h of culture, phosphorylated SMAD 2/3 and SMAD 1/5/9 were observed surrounding and within the cell nuclei of SDSC cultured on high-dose TGF- $\beta$ 3 scaffolds.

$$\frac{M_t}{M_\infty} = 0.006t^{0.25} \quad (R^2 = 0.9955) \quad (2)$$

and fractional release from high-dose scaffolds can be described by:

$$\frac{M_t}{M_\infty} = 0.012t^{0.29} \quad (R^2 = 0.9947) \quad (3)$$

These models were used to predict the total amount of TGF- $\beta$ 3 available to the cells at each time point (Fig. 5B). Evaluation of remaining TGF- $\beta$ 3 in the media after cell culture showed that during the first four days of culture, significantly more TGF- $\beta$ 3 was detected in the high-dose TGF- $\beta$ 3 group compared to the low-dose and exogenous groups (Fig. 5C). The amount of TGF- $\beta$ 3 consumed at each time point was calculated as the difference between the theoretical amount of available TGF- $\beta$ 3 and the remaining amount of TGF- $\beta$ 3 in the media (Fig. 5D). The total amount of TGF- $\beta$ 3 consumed on day 1 was similar among all groups, but higher in the high-dose and exogenous groups compared to the low-dose group at all subsequent time points. While nearly all available TGF- $\beta$ 3 was consumed by cells in the high-dose and exogenous groups at later time points, the percent of total of total available growth factor consumed in the low-dose scaffold group remained at 80% or lower (Fig. 5E).

#### 4. Discussion

Targeted delivery of inductive factors and local maintenance of bioavailability offers a high fidelity and effective regimen for

directing stem cell differentiation and guiding new tissue formation. This study describes a nanofiber-based delivery system that is designed to modulate the local concentration of TGF- $\beta$ 3, promoting biomimetic activation and induction of fibrochondrogenic differentiation of synovium-derived stem cells. Moreover, the production of fibrocartilage-like matrix by SDSC was optimized in a dose-dependent manner.

The ideal scaffold for stem cell-mediated fibrocartilage regeneration must provide not only appropriate physical cues, such as a biomimetic, well-aligned matrix, but should also maintain an effective local concentration of desired inductive factors. This is especially important given the short half-life of TGF- $\beta$  *in vivo* (< 30 minutes) [81,82], the importance of local TGF- $\beta$  concentration on downstream signaling kinetics [111], and the established need for continuous exposure to TGF- $\beta$  over the first week of culture in order to induce stem cell chondrogenesis [83,84]. Within the first 24 hours of culture, it was observed that cells cultured on the TGF- $\beta$ 3-releasing nanofibers exhibited positive staining for phosphorylated SMADs, which are key mediators of TGF- $\beta$  signaling. The TGF- $\beta$  signaling cascade is initiated by binding of TGF- $\beta$  to cell membrane-anchored TGF- $\beta$  type I and type II receptors. These receptors subsequently phosphorylate downstream effectors (SMAD 2/3 or SMAD 1/5/9), which can then form complexes with SMAD 4 and translocate into the nucleus [85–87]. Accumulation of SMADs in the nucleus results in activation or repression of downstream target genes via recruitment of transcriptional co-activators or co-repressors. It is reported that TGF- $\beta$  can induce phosphorylation of both SMAD2/3 and SMAD 1/5/8 in various cell

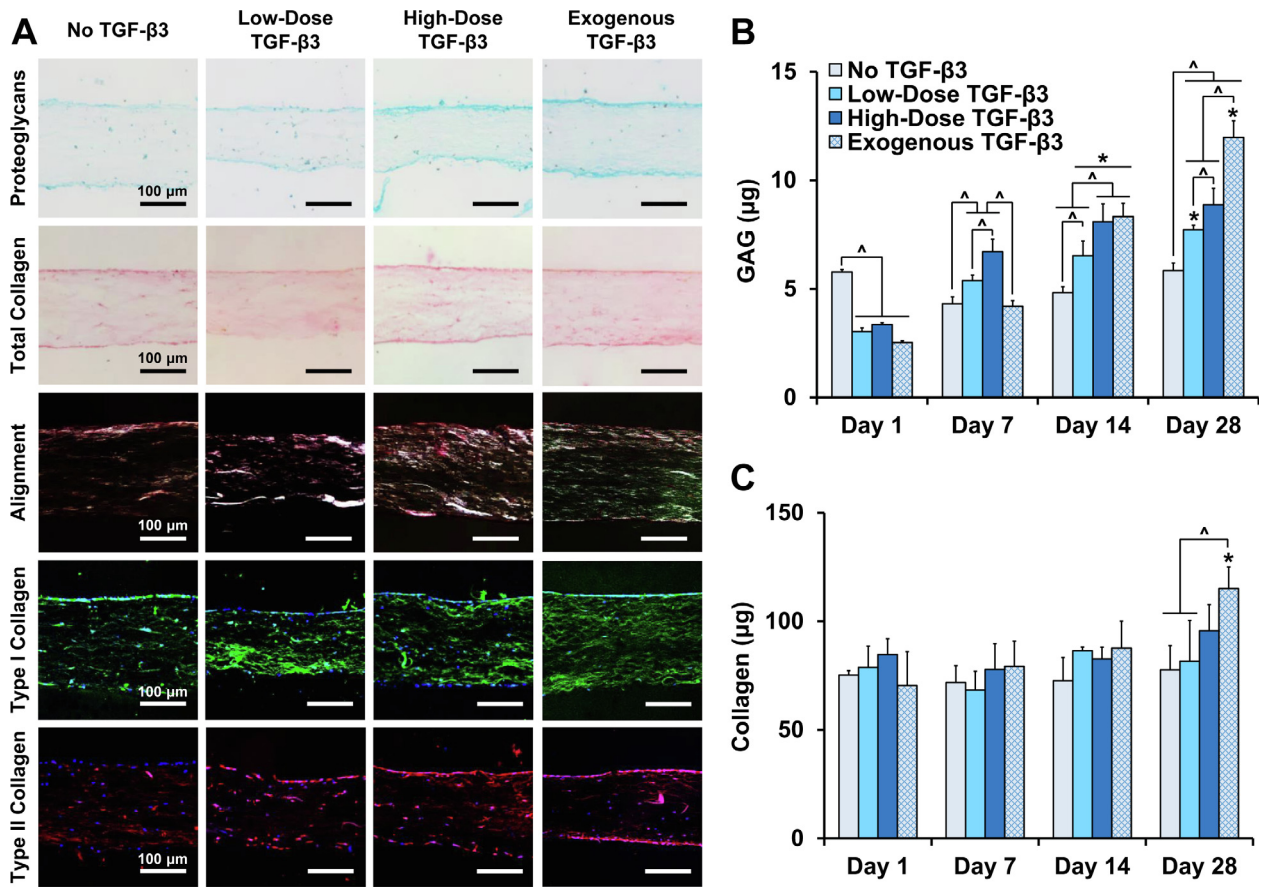


**Fig. 3.** Synthesis of fibrocartilage-like matrix. (A) Cross-sectional view of SDSC-seeded scaffolds after 28 days of culture. Proteoglycan (Alcian blue) and collagen (Picosirius red) deposition were observed in all groups. Polarized light microscopy of Picosirius red-stained sections showed that collagen matrix on scaffold surfaces followed alignment of the underlying scaffold, where areas with similar fiber orientation exhibit similar brightness. While cells were initially seeded only on the top surface of the scaffolds, SDSC penetrated through all scaffolds by day 28 (DAPI). SDSC cultured in the presence of TGF-β3 scaffolds synthesized both type I (green) and type II collagen (pseudo-colored red). Note that only background staining for type II collagen was observed in the control group (see Suppl. Fig. 4), whereas positive staining for type II collagen was found in TGF-β3-stimulated groups. (B) Quantitative evaluation of proteoglycan deposition showed a dose-dependent effect on glycosaminoglycan (GAG) synthesis, with consistently higher GAG deposition on high-dose scaffolds compared to on low-dose scaffolds, and the highest GAG deposition in the exogenous group by day 28 ( $n = 5$ ;  $^{*}p < 0.05$ ). (C) Total collagen synthesis was similar among all groups until day 28, where the highest collagen deposition was observed in the exogenous group ( $n = 5$ ;  $^{*}p < 0.05$ ). Note: compared to the high-dose group, cells in the exogenous group are exposed to approximately 2.5× and 5× more TGF-β3 by day 14 and day 28, respectively;  $^{*}p < 0.05$ , different from previous time point;  $^{\wedge}p < 0.05$ , difference between groups. (For interpretation of the references to color in this figure legend, the reader is referred to the web version of this article.)

types [88,89]. In articular cartilage, canonical TGF-β signaling via SMAD 2/3 is associated with increased proteoglycan synthesis and inhibition of hypertrophy [90,91]. Recently, SMAD 2/3-mediated signaling has been shown to play a similar key role in modulating differentiation potential of progenitor cells derived from meniscal fibrocartilage [92].

In the present study, scaffold-mediated TGF-β3 delivery enhanced cell proliferation at early time points. While TGF-β has varying effects on proliferation in different cell types, its proliferative effects on stem cells are well established [93,94]. In BMSC, it has been shown that TGF-β stimulation induces rapid, SMAD 3-dependent nuclear translocation of β-catenin, a key mediator of the Wnt signaling pathway, which is required for stimulation of BMSC proliferation [93]. Moreover, inhibition of activin receptor-like kinase (ALK) 5, which is the TGF-β type I receptor responsible for activation of SMAD 2/3, slows down BMSC growth [95]. In the present study, SMAD 2/3 activation was observed early on in SDSC cultured on TGF-β3-loaded scaffolds and likely played a similar role in mediating the enhanced proliferation observed at early time points.

Importantly, TGF-β3-releasing scaffolds also supported deposition of fibrocartilage-like matrix by SDSC. Fibrocartilage is uniquely optimized to withstand both tensile and compressive

forces and is characterized by the presence of both types I and II collagen and proteoglycans in the extracellular matrix [8–11]. In the present study, while no significant differences in total collagen synthesis or gene expression were observed, the presence of both types I and II collagen were observed in both TGF-β3 scaffold groups. Previous studies have similarly demonstrated that TGF-β stimulation increases synthesis of type II collagen in chondrocytes [96,97], fibrochondrocytes [92,98], and MSC [99–101] via SMAD 2/3-mediated signaling. Nanofiber-mediated TGF-β3 delivery also significantly enhanced proteoglycan synthesis. Proteoglycans play a critical functional role in cartilaginous tissues wherein they facilitate tissue hydration and swelling, enabling the tissue to withstand compressive forces [102]. It is also well known that TGF-β signaling via SMAD 2/3 enhances proteoglycan synthesis in chondrocytes [97,103,104], fibrochondrocytes [46,105], and MSC [100,101,106]. Collectively, these results suggest that the localized delivery of TGF-β3 from the nanofibers effectively activated chondrogenic induction of SDSC, likely via SMAD-mediated signaling.

Together, these findings demonstrate that the TGF-β3-releasing nanofiber scaffolds developed here effectively guide fibrochondrogenic differentiation of SDSC. While previous studies reported on the use of TGF-β1-releasing fibers for culturing primary fibrochondrocytes [63], to our knowledge, this study is the first to demon-

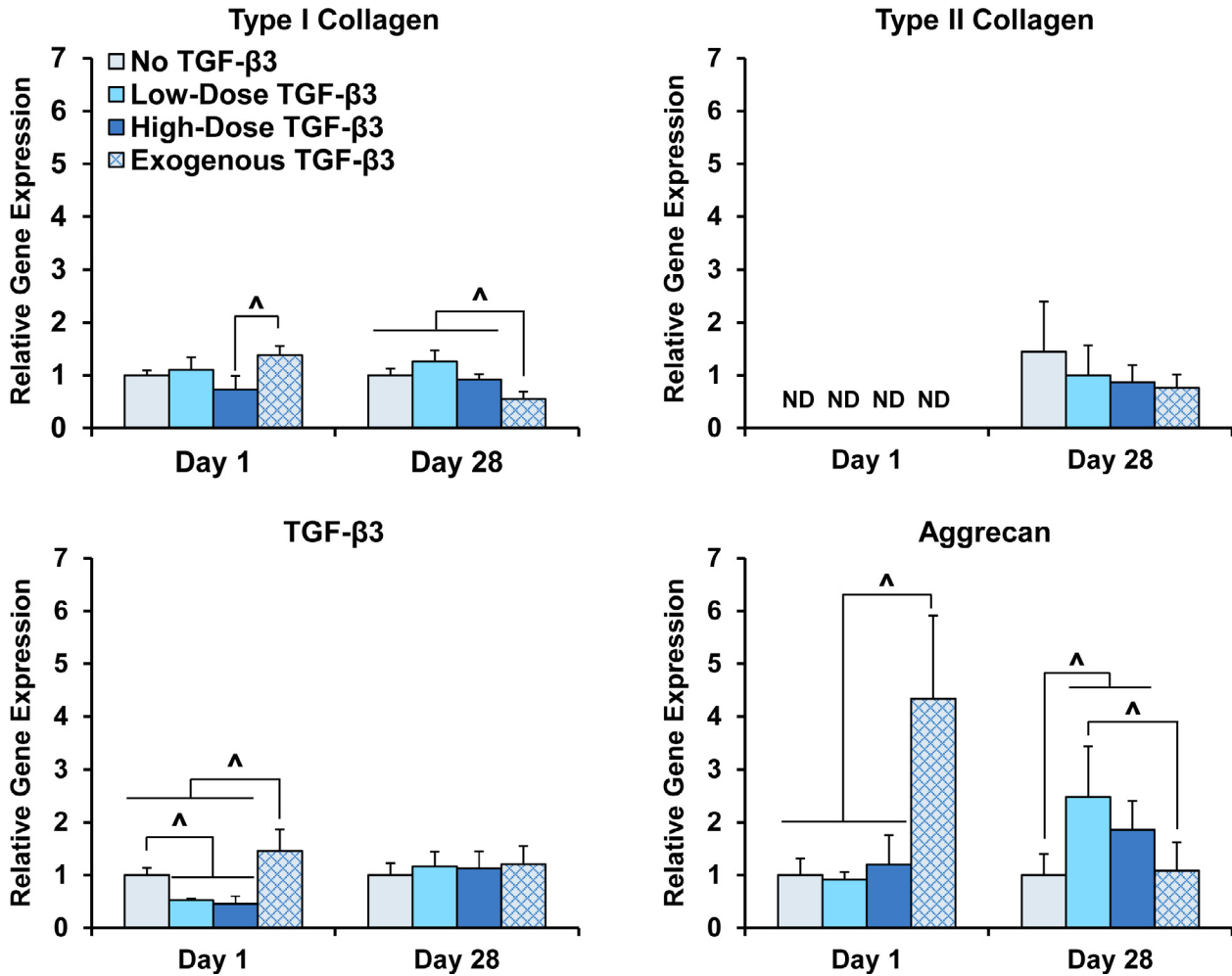


**Fig. 4.** Gene expression. At day 1, expression of type I collagen, TGF-β3, and aggrecan were significantly upregulated in the exogenous TGF-β3 groups compared to control and TGF-β3 scaffold groups ( $n = 5$ ;  $\hat{p} < 0.05$ ). At day 28, type I collagen expression was significantly downregulated in the exogenous group compared to all other groups, aggrecan expression was significantly upregulated on TGF-β3 scaffolds compared to the control and exogenous groups, and no differences in type II collagen or TGF-β3 expression were observed ( $n = 5$ ;  $p < 0.05$ ). *Note:* compared to the high-dose group, cells in the exogenous group are exposed to approximately  $2.5\times$  and  $5\times$  more TGF-β3 by day 14 and day 28, respectively;  $\hat{p} < 0.05$ , difference between groups.

strate the efficacy of nanofiber-mediated TGF-β3 delivery for stem cell fibrochondrogenesis. It has previously been shown that exogenous addition of TGF-β3 combined with aligned PCL nanofibers induces BMSC-mediated formation of a fibrocartilage-like tissue [37]. Subsequently, other studies demonstrated that TGF-β3 and other growth factors can be encapsulated and released from PLGA microspheres embedded in 3D-printed PCL microfiber scaffolds for BMSC-mediated regeneration of meniscal [56] and TMJ [57] fibrocartilage *in vivo*. By incorporating TGF-β3 directly into nanofibers, the present scaffold design not only simplifies the fabrication process, but also increases proximity between seeded cells and the incorporated factors, more closely mimicking the mechanism by which TGF-β is presented to cells in native tissues. *In vivo*, TGF-β is synthesized and secreted in a latent form that is then bound and stored in the extracellular matrix until physiologic loading or other stimuli trigger its release [107]. Here, it was observed that TGF-β3 expression was initially downregulated in cells cultured on TGF-β3-releasing scaffolds compared to cells dosed exogenously with TGF-β3, suggesting that scaffold-provided TGF-β3 may better mimic this process and reduce the need for cellular TGF-β3 synthesis.

In this study, similar to what has been reported for other electrospun delivery systems [108], an initial burst release of TGF-β3

was detected within the first 24 hours of incubation, followed by slower, sustained release. The initial burst release is typically attributed to desorption of growth factor from the fiber surface, while subsequent slower linear release is driven by gradual erosion of the polymer fiber core [108,109]. According to Ritger and Peppas [69], protein release from cylinders can be modeled as an exponential function of time (Eq. (1)), where, in the case of Fickian diffusion from a monodispersion of cylinders, the diffusional exponent  $n$  would be 0.45, i.e.:

$$\frac{M_t}{M_\infty} = kt^{0.45} \quad (4)$$

and  $k = 0.006$  and  $0.012$  for low- and high-dose scaffolds, respectively (see Eqs. (2) and (3)). As shown in Fig. 5A, when  $n$  is set to 0.45, only the first 48 hours of release, during which growth factor is likely predominantly released from the fiber surface, follow Fickian kinetics. Similar deviation from Fickian diffusion have also been reported for β-nerve growth factor delivery from PCL scaffolds [60]. Additionally,  $n$  is known to depend on the aspect ratio of the delivery vehicle and variance in fiber diameter (monodispersed vs. poly-dispersed system). Histogram distributions of fiber diameters for both the low- and high-dose scaffolds are relatively tight, suggesting a monodispersed delivery system. Thus, it is likely that the devi-

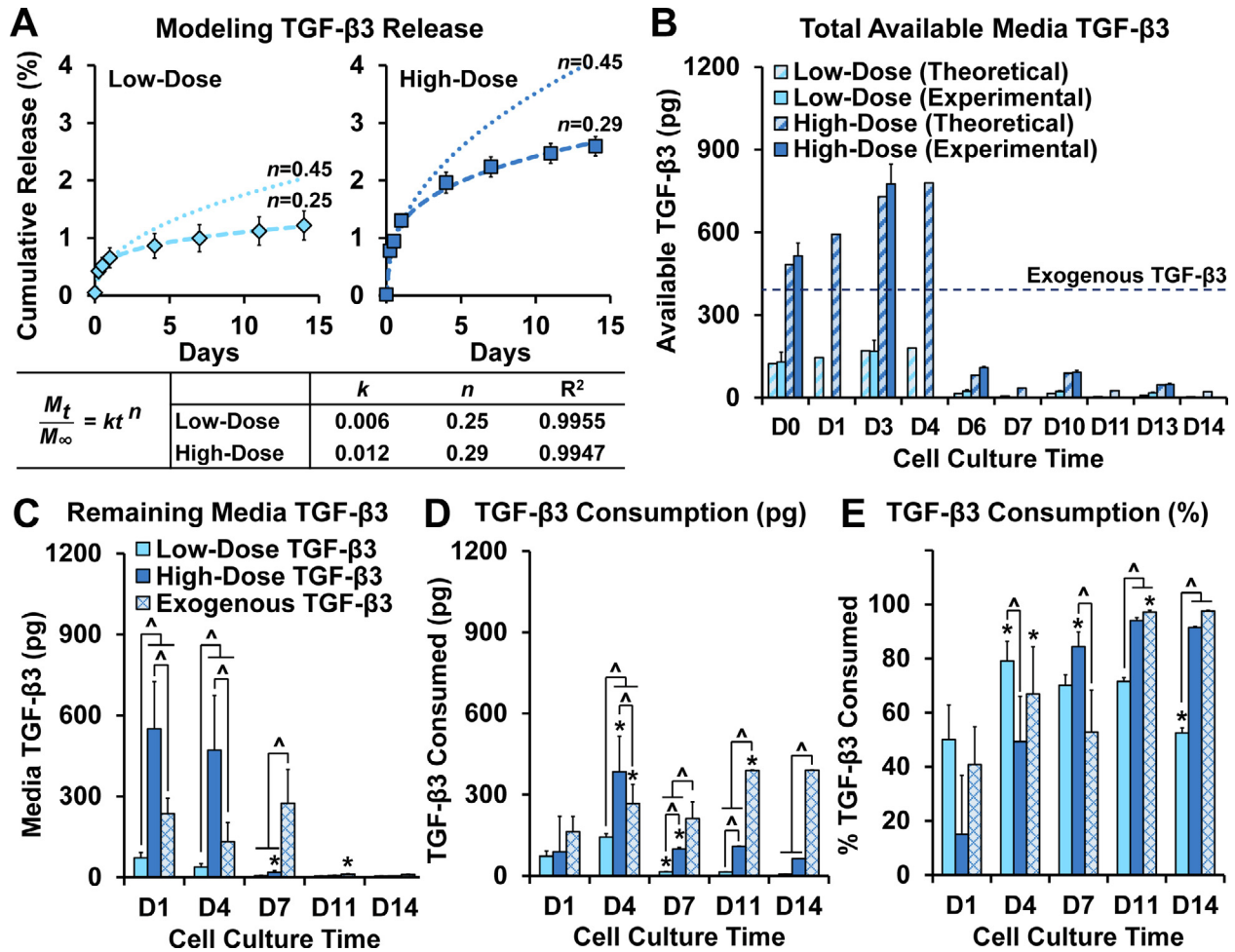


**Fig. 5.** TGF- $\beta$ 3 release and consumption. (A) Fitting the experimental release data to the Ritger-Peppas model ( $M_t/M_\infty$ : fractional release at time  $t$ ;  $k$ : constant;  $n$ : diffusional exponent) showed that the release profiles for both low- and high-dose scaffolds deviate from Fickian diffusion (i.e. where  $n = 0.45$ ). The dotted lines indicate the predicted release based on the model, where the value of  $n$  is as indicated. (B) The models were used to calculate the theoretical amount of TGF- $\beta$ 3 available at each time point of the cell culture study. The dotted horizontal line represents the amount of TGF- $\beta$ 3 available in the exogenous group at each time point. (C) The remaining TGF- $\beta$ 3 detected in the media at each time point ( $n = 5$ ;  $^*p < 0.05$ ) was subtracted from the theoretical amount available to calculate (D) growth factor consumption. A significantly higher amount of TGF- $\beta$ 3 was consumed in the high-dose and exogenous groups compared to in the low-dose groups from day 4 onward. (E) When normalized to the amount of available TGF- $\beta$ 3, it was observed that the percentage of available growth factor initially consumed at day 1 was similar between groups and higher in the low-dose scaffold group on day 4, with the trend reversed at later time points ( $n = 5$ ;  $^*p < 0.05$ ). Note: compared to the high-dose group, cells in the exogenous group are exposed to approximately 2.5 $\times$  and 5 $\times$  more TGF- $\beta$ 3 by day 14 and day 28, respectively;  $^*p < 0.05$ , different from previous time point;  $^\wedge p < 0.05$ , difference between groups.

ation of the experimental diffusional exponent values from the Fickian range may be attributed to the high aspect ratio of the nanofibers compared to conventional cylinders. In agreement with other mechanistic studies of drug release from electrospun PCL nanofibers [61,109], it can be surmised that TGF- $\beta$ 3 release is likely driven by non-Fickian mechanisms. Moreover, the blend of surface and bulk eroding polymers (PCL and PLGA) allows further modulation of factor release from the nanofibers. In particular, blending PLGA with slow-degrading PCL enables continuous, sustained delivery of TGF- $\beta$ 3 for a prolonged period (Suppl. Fig. 6)

Interestingly, fibrochondrogenic response was achieved in this study with a much lower concentration of TGF- $\beta$ 3 than what has previously been reported in studies of fibrochondrogenesis [37,41]. Previous studies have simply used chondrogenic media formulations, which typically comprise 5–10 ng/mL TGF- $\beta$ 3 [17,74,99], and are optimized for formation of hyaline-like cartilage. Contrastingly, in this study, the maximum amount of TGF- $\beta$ 3 released from the high-dose scaffold yielded a 50-fold lower concentration. Analysis of TGF- $\beta$ 3 consumption showed that less than half of the available TGF- $\beta$ 3 was consumed by the cells on the first day of culture, which suggests that a lower dose of

TGF- $\beta$ 3 may be sufficient to enhance SDSC proliferation and induce fibrochondrogenic differentiation. Indeed, in the first two weeks of culture, higher cell proliferation and GAG synthesis were observed on high-dose TGF- $\beta$ 3 scaffolds compared to the exogenous group, even though exogenously stimulated cells were cumulatively exposed to approximately 2.5-times more TGF- $\beta$ 3 compared to the high-dose group by day 14. It is possible that the proximity between TGF- $\beta$ 3 in the scaffold and the seeded cells may result in enhanced bioavailability compared to conventional media supplementation methods, helping to reduce the growth factor dosage requirement. Given the established relationships between local growth factor concentration and cell response [111], future work will seek to elucidate the effects of scaffold-mediated TGF- $\beta$ 3 delivery on local growth factor bioavailability and cell response, including SMAD activation and downstream effects. Additionally, SDSC are known to be more inherently chondrogenic than BMSC [23,25,110], which may also contribute to the overall lower growth factor dose requirement observed.

In summary, this nanoscale delivery system represents an exciting new platform for fibrocartilage interface regeneration, and findings from this study yield critical insights for the regeneration

of other clinically relevant fibrocartilaginous tissues, such as the meniscus and intervertebral disc. Future work will focus on further optimization of the delivery system for exercising temporal and spatial control of protein bioavailability for stem cell differentiation. Additionally, evaluation of the fibrochondrogenic induction potential of this versatile and biomimetic delivery system will be evaluated with more clinically relevant cell types, such as SDSC derived from mature animal models and/or human tissue, as well as testing in *in vivo* models.

## 5. Conclusions

This study focuses on the design and optimization of a nanofiber-based TGF- $\beta$ 3-delivery scaffold and demonstrates its potential for inducing SDSC-mediated fibrocartilage regeneration. Moreover, nanofiber fabrication processes were optimized, specifically to protect the bioactivity of TGF- $\beta$ 3 by co-encapsulation with bovine serum albumin, which resulted in significant enhancement of TGF- $\beta$ 3 release. Nanofiber-mediated localized TGF- $\beta$ 3 delivery enhanced cell proliferation and synthesis of relevant fibrocartilaginous matrix in a dose-dependent manner, with induction achieved at dosages far below exogenous media supplementation.

## Conflicts of interest

All authors have no conflicts of interest.

## Acknowledgements

The authors thank Ms. Hyunji Park for her help with cell culture. This work was supported by the Department of Defense (W81XWH-15-1-0685, HHL), the National Institutes of Health (R01-AR055280, HHL; T32-AR059038, DQ), and the Presidential Early Career Award for Scientists and Engineers (HHL).

## Appendix A. Supplementary data

Supplementary data to this article can be found online at <https://doi.org/10.1016/j.actbio.2019.03.019>.

## References

- [1] R.R. Cooper, S. Misol, Tendon and ligament insertion. A light and electron microscopic study, *J. Bone Joint Surg. Am.* 52 (1970) 1–20.
- [2] M. Benjamin, E.J. Evans, L. Copp, The histology of tendon attachments to bone in man, *J. Anat.* 149 (1986) 89–100.
- [3] S.L. Woo, J. Maynard, D.L. Butler, R.M. Lyon, P.A. Torzilli, W.H. Akeson, R.R. Cooper, B. Oakes, Ligament, tendon, and joint capsule insertions to bone, in: S. L. Woo, J.A. Buckwalter (Eds.), *Injury and Repair of the Musculoskeletal Soft Tissues*, American Academy of Orthopaedic Surgeons, Savannah, GA, 1988, pp. 133–166.
- [4] S.P. Arnoczky, M.E. Adams, K.E. DeHaven, D.R. Eyre, V.C. Mow, The Meniscus, in: S.L.-Y. Woo, J. Buckwalter (Eds.), *Injury and Repair of Musculoskeletal Soft Tissues*, American Academy of Orthopaedic Surgeons, Park Ridge, IL, 1987, pp. 487–537.
- [5] N. Bogduk, L.T. Twomey, *Clinical Anatomy of the Lumbar Spine*, Melbourne, Australia, Churchill Livingstone, 1987.
- [6] D.R. Eyre, P. Benya, J. Buckwalter, B. Caterson, D. Heinegard, T. Oegema, R. Pearce, M. Poe, J. Urban, *Intervertebral Disc. Part B. Basic Science Perspectives*, in: J.W. Frymoyer, S.L. Gordon (Eds.), *New Perspectives on Low Back Pain*, American Academy of Orthopaedic Surgeons, Park Ridge, IL, 1988, pp. 147–207.
- [7] P.J. Sloodweg, H. Muller, Condylar hyperplasia. A clinico-pathological analysis of 22 cases, *J. Maxillofac. Surg.* 14 (1986) 209–214.
- [8] D.R. Eyre, H. Muir, Types I and II collagens in intervertebral disc. Interchanging radial distributions in annulus fibrosus, *Biochem. J* 157 (1976) 267–270.
- [9] H.S. Cheung, Distribution of type I, II, III and V in the pepsin solubilized collagens in bovine menisci, *Connect. Tissue Res* 16 (1987) 343–356.
- [10] J. Kumagai, K. Sarkar, H.K. Uthoff, Y. Okawara, A. Ooshima, Immunohistochemical distribution of type I, II and III collagens in the rabbit supraspinatus tendon insertion, *J. Anat.* 185 (Pt 2) (1994) 279–284.
- [11] S. Thomopoulos, G.R. Williams, J.A. Gimbel, M. Favata, L.J. Soslowsky, Variations of biomechanical, structural, and compositional properties along the tendon to bone insertion site, *J. Orthop. Res.* 21 (2003) 413–419.
- [12] I.E. Wang, S. Mitroo, F.H. Chen, H.H. Lu, S.B. Doty, Age-dependent changes in matrix composition and organization at the ligament-to-bone insertion, *J. Orthop. Res.* 24 (2006) 1745–1755.
- [13] C.S. Proctor, M.B. Schmidt, R.R. Whipple, M.A. Kelly, V.C. Mow, Material properties of the normal medial bovine meniscus, *J. Orthop. Res.* 7 (1989) 771–782.
- [14] J.R. Matyas, M.G. Anton, N.G. Shrive, C.B. Frank, Stress governs tissue phenotype at the femoral insertion of the rabbit MCL, *J. Biomech.* 28 (1995) 147–157.
- [15] J.P. Spalazzi, J. Gallina, S.D. Fung-Kee-Fung, E.E. Konofagou, H.H. Lu, Elastographic imaging of strain distribution in the anterior cruciate ligament and at the ligament-bone insertions, *J. Orthop. Res.* 24 (2006) 2001–2010.
- [16] A.I. Caplan, Mesenchymal stem cells, *J. Orthop. Res.* 9 (1991) 641–650.
- [17] M.F. Pittenger, A.M. Mackay, S.C. Beck, R.K. Jaiswal, R. Douglas, J.D. Mosca, M. A. Moorman, D.W. Simonetti, S. Craig, D.R. Marshak, Multilineage potential of adult human mesenchymal stem cells, *Science* 284 (1999) 143–147.
- [18] A.J. Friedenstein, K.V. Petrakova, A.I. Kurolesova, G.P. Frolova, Heterotopic of bone marrow. Analysis of precursor cells for osteogenic and hematopoietic tissues, *Transplantation* 6 (1968) 230–247.
- [19] H. Nakahara, S.P. Bruder, V.M. Goldberg, A.I. Caplan, *In vivo* osteochondrogenic potential of cultured cells derived from the periosteum, *Clin. Orthop. Relat Res.* (1990) 223–232.
- [20] A. Erices, P. Conget, J.J. Minguell, Mesenchymal progenitor cells in human umbilical cord blood, *Br. J. Haematol.* 109 (2000) 235–242.
- [21] B.C. De, F. Dell'Accio, P. Tylzanowski, F.P. Luyten, Multipotent mesenchymal stem cells from adult human synovial membrane, *Arthritis Rheum.* 44 (2001) 1928–1942.
- [22] P.A. Zuk, M. Zhu, P. Ashjian, D.A. De Ugarte, J.I. Huang, H. Mizuno, Z.C. Alfonso, J.K. Fraser, P. Benhaim, M.H. Hedrick, Human adipose tissue is a source of multipotent stem cells, *Mol. Biol. Cell* 13 (2002) 4279–4295.
- [23] Y. Sakaguchi, I. Sekiya, K. Yagishita, T. Muneta, Comparison of human stem cells derived from various mesenchymal tissues: superiority of synovium as a cell source, *Arthritis Rheum.* 52 (2005) 2521–2529.
- [24] H. Yoshimura, T. Muneta, A. Nimura, A. Yokoyama, H. Koga, I. Sekiya, Comparison of rat mesenchymal stem cells derived from bone marrow, synovium, periosteum, adipose tissue, and muscle, *Cell Tissue Res* 327 (2007) 449–462.
- [25] H. Koga, T. Muneta, T. Nagase, A. Nimura, Y.J. Ju, T. Mochizuki, I. Sekiya, Comparison of mesenchymal tissues-derived stem cells for *in vivo* chondrogenesis: suitable conditions for cell therapy of cartilage defects in rabbit, *Cell Tissue Res.* 333 (2008) 207–215.
- [26] E.B. Hunziker, L.C. Rosenberg, Repair of partial-thickness defects in articular cartilage: cell recruitment from the synovial membrane, *J. Bone Joint Surg. Am.* 78 (1996) 721–733.
- [27] T.B. Kurth, F. Dell'Accio, V. Crouch, A. Augello, P.T. Sharpe, B.C. De, Functional mesenchymal stem cell niches in adult mouse knee joint synovium *in vivo*, *Arthritis Rheum.* 63 (2011) 1289–1300.
- [28] M. Horie, M.D. Driscoll, H.W. Sampson, I. Sekiya, C.T. Caroom, D.J. Prockop, D. B. Thomas, Implantation of allogenic synovial stem cells promotes meniscal regeneration in a rabbit meniscal defect model, *J. Bone Joint Surg. Am.* 94 (2012) 701–712.
- [29] M. Horie, I. Sekiya, T. Muneta, S. Ichinose, K. Matsumoto, H. Saito, T. Murakami, E. Kobayashi, Intra-articular injected synovial stem cells differentiate into meniscal cells directly and promote meniscal regeneration without mobilization to distant organs in rat massive meniscal defect, *Stem Cells* 27 (2009) 878–887.
- [30] D. Hatsushika, T. Muneta, M. Horie, H. Koga, K. Tsuji, I. Sekiya, Intraarticular injection of synovial stem cells promotes meniscal regeneration in a rabbit massive meniscal defect model, *J. Orthop Res* 31 (2013) 1354–1359.
- [31] H. Katagiri, T. Muneta, K. Tsuji, M. Horie, H. Koga, N. Ozeki, E. Kobayashi, I. Sekiya, Transplantation of aggregates of synovial mesenchymal stem cells regenerates meniscus more effectively in a rat massive meniscal defect, *Biochem. Biophys. Res Commun.* 435 (2013) 603–609.
- [32] M. Okuno, T. Muneta, H. Koga, N. Ozeki, Y. Nakagawa, K. Tsuji, S. Yoshiya, I. Sekiya, Meniscus regeneration by syngeneic, minor mismatched, and major mismatched transplantation of synovial mesenchymal stem cells in a rat model, *J. Orthop. Res.* 32 (2014) 928–936.
- [33] Y. Moriguchi, K. Tateishi, W. Ando, K. Shimomura, Y. Yonetani, Y. Tanaka, K. Kita, D.A. Hart, A. Gobbi, K. Shino, H. Yoshikawa, N. Nakamura, Repair of meniscal lesions using a scaffold-free tissue-engineered construct derived from allogenic synovial MSCs in a miniature swine model, *Biomaterials* 34 (2013) 2185–2193.
- [34] D. Hatsushika, T. Muneta, T. Nakamura, M. Horie, H. Koga, Y. Nakagawa, K. Tsuji, S. Hishikawa, E. Kobayashi, I. Sekiya, Repetitive allogeneic intraarticular injections of synovial mesenchymal stem cells promote meniscus regeneration in a porcine massive meniscus defect model, *Osteoarthritis. Cartilage.* 22 (2014) 941–950.
- [35] Y. Segawa, T. Muneta, H. Makino, A. Nimura, T. Mochizuki, Y.J. Ju, Y. Ezura, A. Umezawa, I. Sekiya, Mesenchymal stem cells derived from synovium, meniscus, anterior cruciate ligament, and articular chondrocytes share similar gene expression profiles, *J. Orthop. Res.* 27 (2009) 435–441.
- [36] B.M. Baker, R.L. Mauck, The effect of nanofiber alignment on the maturation of engineered meniscus constructs, *Biomaterials* 28 (2007) 1967–1977.

- [37] B.M. Baker, R.P. Shah, A.H. Huang, R.L. Mauck, Dynamic tensile loading improves the functional properties of mesenchymal stem cell-laden nanofiber-based fibrocartilage, *Tissue Eng. Pt. A* 17 (2011) 1445–1455.
- [38] D.B. Fox, J.J. Warnock, A.M. Stoker, J.K. Luther, M. Cockrell, Effects of growth factors on equine synovial fibroblasts seeded on synthetic scaffolds for avascular meniscal tissue engineering, *Res. Vet. Sci.* 88 (2010) 326–332.
- [39] Y. Tan, Y. Zhang, M. Pei, Meniscus reconstruction through coculturing meniscus cells with synovium-derived stem cells on small intestine submucosa—a pilot study to engineer meniscus tissue constructs, *Tissue Eng. Pt. A* 16 (2010) 67–79.
- [40] J.T. Connelly, E.J. Vanderploeg, J.K. Mouw, C.G. Wilson, M.E. Levenston, Tensile loading modulates bone marrow stromal cell differentiation and the development of engineered fibrocartilage constructs, *Tissue Eng. Pt. A* 16 (2010) 1913–1923.
- [41] S. Thomopoulos, R. Das, V. Birman, L. Smith, K. Ku, E.L. Elson, K.M. Pryse, J.P. Marquez, G.M. Genin, Fibrocartilage tissue engineering: the role of the stress environment on cell morphology and matrix expression, *Tissue Eng. Pt. A* 17 (2011) 1039–1053.
- [42] E. Blitz, A. Sharir, H. Akiyama, E. Zelzer, Tendon-bone attachment unit is formed modularly by a distinct pool of Scx- and Sox9-positive progenitors, *Development* 140 (2013) 2680–2690.
- [43] B.H. Thorp, I. Anderson, S.B. Jakowlew, Transforming growth factor-beta 1, -beta 2 and -beta 3 in cartilage and bone cells during endochondral ossification in the chick, *Development* 114 (1992) 907.
- [44] A. Tekari, R. Luginbuehl, W. Hofstetter, R.J. Egli, Transforming growth factor beta signaling is essential for the autonomous formation of cartilage-like tissue by expanded chondrocytes, *PLoS One* 10 (2015) e0120857.
- [45] W. Madej, C.A. van, D.E. Blaney, P. Buma, P.M. van der Kraan, Unloading results in rapid loss of TGFbeta signaling in articular cartilage: role of loading-induced TGFbeta signaling in maintenance of articular chondrocyte phenotype?, *Osteoarthritis Cartilage* 24 (2016) 1807–1815.
- [46] S. Collier, P. Ghosh, Effects of transforming growth factor beta on proteoglycan synthesis by cell and explant cultures derived from the knee joint meniscus, *Osteoarthr. Cartilage* 3 (1995) 127–138.
- [47] R. Landesberg, E. Takeuchi, J.E. Puzas, Cellular, biochemical and molecular characterization of the bovine temporomandibular joint disc, *Arch. Oral Biol.* 41 (1996) 761–767.
- [48] S.M. Imler, A.N. Doshi, M.E. Levenston, Combined effects of growth factors and static mechanical compression on meniscus explant biosynthesis, *Osteoarthr. Cartilage* 12 (2004) 736–744.
- [49] S.A. Lietman, W. Hobbs, N. Inoue, A.H. Reddi, Effects of selected growth factors on porcine meniscus in chemically defined medium, *Orthopedics* 26 (2003) 799–803.
- [50] C.A. Pangborn, K.A. Athanasiou, Growth factors and fibrochondrocytes in scaffolds, *J. Orthop. Res.* 23 (2005) 1184–1190.
- [51] M.S. Detamore, K.A. Athanasiou, Evaluation of three growth factors for TMJ disc tissue engineering, *Ann. Biomed. Eng.* 33 (2005) 383–390.
- [52] O. Guillaume, S.M. Naqvi, K. Lennon, C.T. Buckley, Enhancing cell migration in shape-memory alginate-collagen composite scaffolds: in vitro and ex vivo assessment for intervertebral disc repair, *J. Biomater. Appl.* 29 (2015) 1230–1246.
- [53] L. Galatz, S. Rothermich, K. Vanderploeg, B. Petersen, L. Sandell, S. Thomopoulos, Development of the supraspinatus tendon-to-bone insertion: localized expression of extracellular matrix and growth factor genes, *J. Orthop. Res.* 25 (2007) 1621–1628.
- [54] C.N. Manning, H.M. Kim, S. Sakiyama-Elbert, L.M. Galatz, N. Havlioglu, S. Thomopoulos, Sustained delivery of transforming growth factor beta three enhances tendon-to-bone healing in a rat model, *J. Orthop. Res.* 29 (2011) 1099–1105.
- [55] J.P. Spalazzi, M.C. Vyner, M.T. Jacobs, K.L. Moffat, H.H. Lu, Mechanoactive scaffold induces tendon remodeling and expression of fibrocartilage markers, *Clin. Orthop. Relat. Res.* 466 (2008) 1938–1948.
- [56] C.H. Lee, S.A. Rodeo, L.A. Fortier, C. Lu, C. Eriskin, J.J. Mao, Protein-releasing polymeric scaffolds induce fibrochondrocytic differentiation of endogenous cells for knee meniscus regeneration in sheep, *Sci. Transl. Med.* 6 (2014) 266ra171.
- [57] S. Tarafder, A. Koch, Y. Jun, C. Chou, M.R. Awadallah, C.H. Lee, Micro-precise spatiotemporal delivery system embedded in 3D printing for complex tissue regeneration, *Biofabrication* 8 (2016) 025003.
- [58] K.L. Moffat, A.S. Kwei, J.P. Spalazzi, S.B. Doty, W.N. Levine, H.H. Lu, Novel nanofiber-based scaffold for rotator cuff repair and augmentation, *Tissue Eng. Pt. A* 15 (2009) 115–126.
- [59] S.D. Subramony, B.R. Dargis, M. Castillo, E.U. Azeloglu, M.S. Tracey, A. Su, H.H. Lu, The guidance of stem cell differentiation by substrate alignment and mechanical stimulation, *Biomaterials* 34 (2013) 1942–1953.
- [60] S.Y. Chew, J. Wen, E.K. Yim, K.W. Leong, Sustained release of proteins from electrospun biodegradable fibers, *Biomacromolecules* 6 (2005) 2017–2024.
- [61] C.M. Valmikinathan, S. Defroda, X. Yu, Polycaprolactone and bovine serum albumin based nanofibers for controlled release of nerve growth factor, *Biomacromolecules* 10 (2009) 1084–1089.
- [62] F. Qu, J.L. Holloway, J.L. Esterhai, J.A. Burdick, R.L. Mauck, Programmed biomolecule delivery to enable and direct cell migration for connective tissue repair, *Nat. Commun.* 8 (2017) 1780.
- [63] G. Vadala, P. Mozetic, A. Rainer, M. Centola, M. Loppini, M. Trombetta, V. Denaro, Bioactive electrospun scaffold for annulus fibrosus repair and regeneration, *Eur. Spine J.* 21 (Suppl 1) (2012) S20–S26.
- [64] Z. Man, L. Yin, Z. Shao, X. Zhang, X. Hu, J. Zhu, L. Dai, H. Huang, L. Yuan, C. Zhou, H. Chen, Y. Ao, The effects of co-delivery of BMSC-affinity peptide and rhTGF-β1 from coaxial electrospun scaffolds on chondrogenic differentiation, *Biomaterials* 35 (2014) 5250–5260.
- [65] D.F.G. Remst, E.N. Blaney Davidson, E.L. Vitters, R.A. Bank, W.B. van den Berg, P.M., van der Kraan, TGF-β induces Lysyl hydroxylase 2b in human synovial osteoarthritic fibroblasts through ALK5 signaling, *Cell Tissue Res.* 355 (2014) 163–171.
- [66] D.H. Reneker, I. Chun, Nanometre diameter fibres of polymer, produced by electrospinning, *Nanotechnology* 7 (1996) 216–223.
- [67] C. Eriskin, X. Zhang, H.H. Lu, Controlled release of TGF-β3 from nanofibers, its stability and bioactivity against chondrocytes, *Trans. Orthop. Res. Soc.* (2011).
- [68] N.M. Lee, C. Eriskin, T. Iskratsch, M. Sheetz, W.N. Levine, H.H. Lu, Polymer fiber-based models of connective tissue repair and healing, *Biomaterials* 112 (2017) 303–312.
- [69] P.L. Ritger, N.A. Peppas, A simple equation for description of solute release I. Fickian and non-fickian release from non-swellable devices in the form of slabs, spheres, cylinders or discs, *J. Control. Release* 5 (1) (1987) 23–36.
- [70] S.R. Sampat, G.D. O'Connell, J.V. Fong, E. Egre-Aguaron, G.A. Ateshian, C.T. Hung, Growth factor priming of synovium-derived stem cells for cartilage tissue engineering, *Tissue Eng Part A* 17 (2011) 2259–2265.
- [71] T. Zimmermann, E. Kunisch, R. Pfeiffer, A. Hirth, H.D. Stahl, U. Sack, A. Laube, E. Liesaus, A. Roth, E. Palombo-Kinne, F. Emmrich, R.W. Kinne, Isolation and characterization of rheumatoid arthritis synovial fibroblasts from primary culture—primary culture cells markedly differ from fourth-passage cells, *Arthritis Res.* 3 (2001) 72–76.
- [72] A.R. Tan, E. Egre-Aguaron, G.D. O'Connell, C.D. Vandenberg, R.K. Aaron, G. Vunjak-Novakovic, J.C. Bulinski, G.A. Ateshian, C.T. Hung, Passage-dependent relationship between mesenchymal stem cell mobilization and chondrogenic potential, *Osteoarthr. Cartilage* 23 (2015) 319–327.
- [73] N. Jaiswal, S.E. Haynesworth, A.I. Caplan, S.P. Bruder, Osteogenic differentiation of purified, culture-expanded human mesenchymal stem cells in vitro, *J. Cell Biochem.* 64 (1997) 295–312.
- [74] A.M. Mackay, S.C. Beck, J.M. Murphy, F.P. Barry, C.O. Chichester, M.F. Pittenger, Chondrogenic differentiation of cultured human mesenchymal stem cells from marrow, *Tissue Eng* 4 (1998) 415–428.
- [75] R.W. Farndale, C.A. Sayers, A.J. Barrett, A direct spectrophotometric microassay for sulfated glycosaminoglycans in cartilage cultures, *Connect. Tissue Res* 9 (1982) 247–248.
- [76] B.O. Enobakhare, D.L. Bader, D.A. Lee, Quantification of sulfated glycosaminoglycans in chondrocyte/alginate cultures, by use of 1,9-dimethylmethylene blue, *Anal. Biochem.* 243 (1996) 189–191.
- [77] G.K. Reddy, C.S. Enwemeka, A simplified method for the analysis of hydroxyproline in biological tissues, *Clin. Biochem.* 29 (1996) 225–229.
- [78] G. Landemore, M. Quillec, N. Oulhaj, J. Izard, Collagen-associated sulphated proteoglycans. Ultrastructure after formaldehyde-cetylpyridinium chloride fixation, *Histochem. J* 23 (1991) 534–540.
- [79] E.B. Hunziker, A. Ludi, W. Herrmann, Preservation of cartilage matrix proteoglycans using cationic dyes chemically related to ruthenium hexaammine trichloride, *J. Histochem. Cytochem.* 40 (1992) 909–917.
- [80] N.T. Khanarian, J. Jiang, L.Q. Wan, V.C. Mow, H.H. Lu, A hydrogel-mineral composite scaffold for osteochondral interface tissue engineering, *Tissue Eng. Pt. A* 18 (2012) 533–545.
- [81] R.J. Coffey, W.E. Russell, J.A. Barnard, Pharmacokinetics of TGFβ with Emphasis on Effects in Liver and Gut, *ANYAS* 593 (1990) 285–291.
- [82] J.R. Dasch, W.O. Waegell, K. Karroll, D.R. Pace, L.E. Ellingsworth, Capture Immunoassays Specific for TGFβ1 and TGFβ2: Use in Pharmacokinetic Studies, *ANYAS* 593 (1990) 303–305.
- [83] A.T. Mehlhorn, H. Schmal, S. Kaiser, G. Lepski, G. Finkenzeller, G.B. Stark, N.T. Südkamp, Mesenchymal stem cells maintain TGF-β-mediated chondrogenic phenotype in alginate bead culture, *Tissue Eng.* 12 (2006) 1393–1403.
- [84] L. Bian, D.Y. Zhai, E. Tous, R. Rai, R.L. Mauck, J.A. Burdick, Enhanced MSC chondrogenesis following delivery of TGF-beta3 from alginate microspheres within hyaluronic acid hydrogels in vitro and in vivo, *Biomaterials* 32 (2011) 6425–6434.
- [85] C.H. Heldin, K. Miyazono, D.P. Ten, TGF-beta signalling from cell membrane to nucleus through SMAD proteins, *Nature* 390 (1997) 465–471.
- [86] R. Derynck, Y. Zhang, X.H. Feng, Transcriptional activators of TGF-β responses: smads, *Cell* 95 (1998) 737–740.
- [87] J. Massague, TGF-β signal transduction, *Annu. Rev. Biochem.* 67 (1998) 753–791.
- [88] K.H. Wrighton, X. Lin, P.B. Yu, X.H. Feng, Transforming growth factor β can stimulate smad1 phosphorylation independently of bone morphogenic protein receptors, *J. Biol. Chem.* 284 (2009) 9755–9763.
- [89] E. Grönroos, I.J. Kingston, A. Ramachandran, R.A. Randall, P. Vizán, C.S. Hill, Transforming Growth Factor β Inhibits Bone Morphogenetic Protein-Induced Transcription through Novel Phosphorylated Smad1/5-Smad3 Complexes, *Mol. Cell. Biol.* 32 (2012) 2904.
- [90] C.M. Ferguson, E.M. Schwarz, P.R. Reynolds, J.E. Puzas, R.N. Rosier, R.J. O'Keefe, Smad2 and 3 mediate transforming growth factor-beta1-induced inhibition of chondrocyte maturation, *Endocrinology* 141 (2000) 4728–4735.
- [91] T.F. Li, M. Darowish, M.J. Zusick, D. Chen, E.M. Schwarz, R.N. Rosier, H. Drissi, R.J. O'Keefe, Smad3-deficient chondrocytes have enhanced BMP signaling and accelerated differentiation, *J. Bone Miner. Res.* 21 (2006) 4–16.
- [92] H. Muhammad, B. Schminke, C. Bode, M. Roth, J. Albert, S. von der Heyde, V. Rosen, N. Miosge, Human migratory meniscus progenitor cells are controlled via the TGF-β pathway, *Stem Cell Rep.* 3 (2014) 789–803.

- [93] H. Jian, X. Shen, I. Liu, M. Semenov, X. He, X.F. Wang, Smad3-dependent nuclear translocation of  $\beta$ -catenin is required for TGF- $\beta$ 1-induced proliferation of bone marrow-derived adult human mesenchymal stem cells, *Genes Dev.* 20 (2006) 666–674.
- [94] A.A. Worster, B.D. Brower-Toland, L.A. Fortier, S.J. Bent, J. Williams, A.J. Nixon, Chondrocytic differentiation of mesenchymal stem cells sequentially exposed to transforming growth factor-beta1 in monolayer and insulin-like growth factor-I in a three-dimensional matrix, *J. Orthop. Res.* 19 (2001) 738–749.
- [95] F. Ng, S. Boucher, S. Koh, K.S.R. Sastry, L. Chase, U. Lakshmiathy, C. Choong, Z. Yang, M.C. Vemuri, M.S. Rao, V. Tanavde, PDGF, TGF- $\beta$ , and FGF signaling is important for differentiation and growth of mesenchymal stem cells (MSCs): transcriptional profiling can identify markers and signaling pathways important in differentiation of MSCs into adipogenic, chondrogenic, and osteogenic lineages, *Blood* 112 (2008) 295.
- [96] A. Frazer, R.A.D. Bunning, M. Thavarajah, J.M. Seid, R.G. Russell, Studies on type II collagen and aggrecan production in human articular chondrocytes in vitro and effects of transforming growth factor- $\beta$  and interleukin-1 $\beta$ , *Osteoarthr. Cartilage* 2 (1994) 235–245.
- [97] Y. Zhu, H. Tao, C. Jin, Y. Liu, X. Lu, X. Hu, X. Wang, Transforming growth factor-beta1 induces type II collagen and aggrecan expression via activation of extracellular signal-regulated kinase 1/2 and Smad2/3 signaling pathways, *Mol. Med Rep.* 12 (2015) 5573–5579.
- [98] T. Furumatsu, T. Kanazawa, Y. Yokoyama, N. Abe, T. Ozaki, Inner meniscus cells maintain higher chondrogenic phenotype compared with outer meniscus cells, *Connect. Tissue Res* 52 (2011) 459–465.
- [99] A.A. Worster, A.J. Nixon, B.D. Brower-Toland, J. Williams, Effect of transforming growth factor beta1 on chondrogenic differentiation of cultured equine mesenchymal stem cells, *Am. J. Vet. Res.* 61 (2000) 1003–1010.
- [100] K. Miyanishi, M.C. Trindade, D.P. Lindsey, G.S. Beaupre, D.R. Carter, S.B. Goodman, D.J. Schurman, R.L. Smith, Effects of hydrostatic pressure and transforming growth factor-beta 3 on adult human mesenchymal stem cell chondrogenesis in vitro, *Tissue Eng* 12 (2006) 1419–1428.
- [101] E. Steck, H. Bertram, R. Abel, B. Chen, A. Winter, W. Richter, Induction of intervertebral disc-like cells from adult mesenchymal stem cells, *Stem Cells* 23 (2009) 403–411.
- [102] M. Yanagishita, Function of proteoglycans in the extracellular matrix, *Acta Pathol. Jpn.* 43 (1993) 283–293.
- [103] T.I. Morales, A.B. Roberts, Transforming growth factor beta regulates the metabolism of proteoglycans in bovine cartilage organ cultures, *J. Biol. Chem.* 263 (1988) 12828–12831.
- [104] T.I. Morales, M.E. Joyce, M.E. Sobel, D. Danielpour, A.B. Roberts, Transforming growth factor-beta in calf articular cartilage organ cultures: synthesis and distribution, *Arch. Biochem. Biophys.* 288 (1991) 397–405.
- [105] C.G. Wilson, J.F. Nishimuta, M.E. Levenston, Chondrocytes and Meniscal Fibrochondrocytes Differentially Process Aggrecan During De Novo Extracellular Matrix Assembly, A In Press, *Tissue Eng. Pt.* 2009.
- [106] F. Barry, R.E. Boynton, B. Liu, J.M. Murphy, Chondrogenic differentiation of mesenchymal stem cells from bone marrow: differentiation-dependent gene expression of matrix components, *Exp. Cell Res.* 268 (2001) 189–200.
- [107] J.S. Munger, J.G. Harpel, P.E. Gleizes, R. Mazzieri, I. Nunes, D.B. Rifkin, Latent transforming growth factor- $\beta$ : Structural features and mechanisms of activation, *Kidney Int.* 51 (1997) 1376–1382.
- [108] W. Ji, Y. Sun, F. Yang, J.J.P. van den Beucken, M. Fan, Z. Chen, J.A. Jansen, Bioactive electrospun scaffolds delivering growth factors and genes for tissue engineering applications, *Pharm. Res.* 28 (2011) 1259–1272.
- [109] R. Srikar, A.L. Yarin, C.M. Megaridis, A.V. Bazilevsky, E. Kelley, Desorption-limited mechanism of release from polymer nanofibers, *Langmuir* 24 (2008) 965–974.
- [110] S. Shirasawa, I. Sekiya, Y. Sakaguchi, K. Yagishita, S. Ichinose, T. Muneta, In vitro chondrogenesis of human synovium-derived mesenchymal stem cells: optimal condition and comparison with bone marrow-derived cells, *J. Cell Biochem.* 97 (2006) 84–97.
- [111] D.C. Clarke, M.L. Brown, R.A. Erickson, Y. Shi, X. Liu, Transforming growth factor beta depletion is the primary determinant of Smad signaling kinetics, *Mol Cell Biol.* 29 (2009) 2443–2455.